

Preparation of Acetylated Chitosan/Carbonated Hydroxyapatite Composite Barriers for Guided Bone Regeneration

Sang Min Park and Hong Sung Kim*

Department of Biomaterial Science, Pusan National University, Miryang-si, Gyeongnam 50463, Korea

Received August 11, 2016; Revised October 20, 2016; Accepted October 31, 2016

Abstract: Biopolymer/bioceramic composites were prepared by blending acetylated chitosan (ACS) with carbonated nano-size hydroxyapatite (CHAP) for use as a guided tissue regeneration barrier. The carbonate group of CHAP was a partial substitution of the hydroxyl group and/or phosphate group of hydroxyapatite by sintering with carbon dioxide. Chitosan/CHAP composites were acetylated with acetic anhydride to form the ACS/CHAP composites. The compositions and properties of the composites were confirmed by Fourier transform infrared spectroscopy, inductively coupled plasma mass spectrometry, zeta potential analysis, X-ray diffraction analysis, universal testing machine analysis, scanning electron microscopy, 3-(4,5-dimethylthiazol-2-yl)-2,5-diphenyltetrazolium bromide (MTT) assay, *etc.* The surface energies of the composites were increased by carbonation and acetylation. The acetylation of chitosan increased the lysozyme degradation of the composite. The carbonation of hydroxyapatite significantly improved the viability of osteoblast-like cell on the composite. The high viability and intact phenotype of cell occurred on composite with ACS/CHAP ratio of 50/50, which had sufficient elastic modulus for a guided bone regeneration barrier.

Keywords: acetylated chitosan, carbonated hydroxyapatite, composite, GBR barrier.

Introduction

Guided bone regeneration (GBR) is a common procedure used for guiding the tissue regeneration of periodontal bone. In this method, membrane barriers are used to cover bone defects and to block the invasion of surrounding soft tissues.¹ This provides sufficient time for the osteogenic cells from bone marrow to proliferate and form new bony tissues.² Membrane barriers for GBR are currently made of resorbable materials, because non-resorbable membranes have to be removed through a second surgical procedure after bone regeneration. The ideal material for the barrier should have biocompatibility, biodegradability, osteoconductivity, and appropriate mechanical properties.³

Chitin, the second most abundant natural biopolymer, is commonly found in the shells of marine crustaceans and in the cell walls of fungi. Chitosan (CS) is obtained through partial N-deacetylation of chitin, and is composed of glucosamine and N-acetyl glucosamine units with β -1,4-glucosidic linkage.⁴ Since CS possesses an easy-to-shape property, biodegradability, biocompatibility, and low toxicity, it has received much attention in the field of biomedical research for applications such as wound dressing, a drug delivery vehicle, and a tissue engineering scaffold.^{5,6} In particular, it has been researched for bone, blood vessel, and nerve tissue engineering owing to its wound healing promotion effect by stimulating inflammatory cells and

its inhibitory effect on bacterial growth.⁷

Hydroxyapatite (HAP), $[\text{Ca}_{10}(\text{PO}_4)_6(\text{OH})_2]$, is an inorganic component of natural bone. HAP particles have been used commercially in dental field for periodontal tissue regeneration, in forms such as particles, pastes, cements, and coating agents. The problems with HAP particle include its brittle and mobile ceramic nature, making it difficult to apply as a GBR barrier material.^{3,8}

Therefore HAP has been used in composite with polymers such as chitosan,⁹ poly(lactic acid),¹⁰ polycaprolactone¹¹ for guided tissue regeneration. The chitosan/HAP composite was examined because of the relative biocompatibility of chitosan as naturally occurring substance and the advantage of promoting the tissue regeneration.^{12,13} However chitosan can often lead to an over-expressed inflammatory response,¹⁴ and the alkali surface of HAP particles often causes damage to the surrounding tissues and/or occasionally increases acute inflammation at the implant site.¹⁵

In this study, carbonated HAP was designed to mimic the surface of the natural bone and to improve its biocompatibility and osteoconductivity. Acetylated CS (ACS) was prepared by conversion of the glucosamine to N-acetyl glucosamine in order to mimic the surface of chitin for inducing a relatively mild inflammatory response. The composites were composed of the acetylated CS matrix with the carbonated HAP nanoparticles. The physical and biological properties of the composites were investigated for application as a GBR barrier.

*Corresponding Author. E-mail: khs@pusan.ac.kr

Experimental

Materials. Chitosan was obtained from Taehoon-bio Corp. (Korea) and purified with 2 wt% aqueous acetic acid and 5 wt% sodium hydroxide solution. Its degree of deacetylation was 97% and its weight-average molecular weight was approx. 400,000. HAP nanopowder, with an average particle size of less than 200 nm, was obtained from Sigma-Aldrich Corp. (USA). The stoichiometric Ca/P ratio of the nanopowder was about 1.79, which was confirmed using inductively coupled plasma mass spectrometry (ICP-MS). Egg-white lysozyme, phosphate buffered saline (PBS), and 3-(4,5-dimethylthiazol-2-yl)-2,5-diphenyl tetrazolium bromide (MTT) were purchased from Sigma-Aldrich Corp. (USA). Acetic anhydride, acetic acid, methanol (MeOH), and sodium hydroxide (NaOH) were used at a guaranteed reagent grade without further purification.

Synthesis of Carbonated Hydroxyapatite. The HAP nanopowder was treated under a dry CO₂ atmosphere for 48 h at 900 °C in an electric furnace. Table I shows the specifications for the specimens. In this carbonation process, the carbonate group partially replaced the hydroxyl group and/or phosphate group of HAP. The carbonated hydroxyapatite (CHAP) was analyzed by Fourier transform infrared spectroscopy (FTIR), ICP-MS, zeta potential analysis, and X-ray diffraction analysis (XRD).

Preparation of Composites. The CS/CHAP composites were prepared as follows. CHAP was uniformly dispersed in a 2 wt% acetic acid solution at desired concentration, using an ultrasonic mixer. Then, 3 wt% CS was dissolved in the CHAP-dispersed solution. The weight ratios of CS/CHAP composites in the solution were 100/0, 70/30, 50/50, 30/70, respectively. The composites were solidified in 10 wt% NaOH solution after casting on a glass plate. The fabricated composites of film type were washed several times with distilled water and then dried slowly at room temperature.

Acetylation of Composites. The CS/CHAP composites were reacted with 1.0 M acetic anhydride in MeOH solution for acetylation. The reactions were carried out with stirring at 120 rpm, at 25 °C for 24 h. After the reaction, the composites were washed with MeOH solution to remove unreacted acetic anhydride and byproducts. The amino groups on the surface of the composite were replaced with acetamide groups by the acetylation.

Instrumental Analyses. The stoichiometric Ca/P ratio of the bioceramic particles, HAP and CHAP, were obtained by ICP-MS (iCAP 6200; Thermo Scientific, USA). The zeta poten-

tial of the dispersed bioceramic particles was measured with a zeta potential analyzer (ELS-Z2; Otsuka Electronics Corp., Japan).

The X-ray diffractogram was recorded by X-ray diffractometer (DMAX 2000V; Rigaku Corp., Japan) using the reflection method with monochromatic CuK α radiation at 40 kV, 30 mA, and a scan speed of 10°/min.

The FTIR spectrum was measured in a FTIR spectrometer (IRAffinity-1; Shimadzu Corp., Japan) at a wavelength range of 400-4000 cm⁻¹ by the KBr pellet method.

The contact angle of the composites was measured with a contact angle meter (AMS2001 G-1; Mirero System, Korea) at 23 °C by the sessile drop method using deionized water.

The cell morphology was observed by scanning electron microscopy (SEM; HITACHI-S3500N; Hitachi Corp., Japan), after culturing the cells (1.5×10⁴ cells/well) on the composites for 3 days. The cells were immobilized on its intact location in the composites by pre-treatment with glutaraldehyde, OsO₄, and 1,1,1,3,3,3-hexamethyl disilazane solution, respectively. The composites were coated with gold using an ion sputter for obtaining a clear image.

Mechanical properties were measured by a universal testing machine (UTM; SSTM-1; United Corp., USA) at a load cell of 5 kg and tensile speed of 5 mm/min. The specimen size was 5 mm×40 mm, and the average value was obtained from five repeated measurements.

Water Absorption and Biodegradation. The composites were immersed in 0.01 M PBS for 2 h at 20 °C, following which surface water was removed, and the composites were then weighed and marked as W_1 . The water absorption was determined by the equation $(W_1 - W_0)/W_0 \times 100\%$, where W_0 is the dry weight of the specimen. To determine the enzymatic biodegradation of the composites *in vitro*, the composites were immersed in 0.1 M PBS solution containing 4 mg/mL lysozyme at pH 6.6 and 37 °C for 3, 6, 10, 14, and 17 days. The composites were removed from the PBS solution, dried, and weighed.

Cell Viability Assay. Cell viability was estimated by the MTT assay. The osteosarcoma MG-63 cell line was obtained from Korea Cell Line Bank (KCLB; Seoul, Korea) and maintained in Dulbecco's minimum essential medium (DMEM; GIBCO BRL, Grand Island, NY, USA) containing 10% fetal bovine serum (GIBCO BRL) and 1% streptomycin (GIBCO BRL). The cells (1.5×10⁴ cells/well) were incubated for 3 days in 96-well plates under a humidified atmosphere containing 5% CO₂. Thereafter, the medium in the plates was removed,

Table I. Specifications of the HAP and Carbonated HAP (CHAP) Particles

	CO ₂ Supply Rate	Reaction Time	Degree of Carbonation	Zeta Potential (mV)	Ca/P
HAP	-	-	non	+1.14	1.796
Intergrade-CHAP	0.5 L/min	48 h	half	-11.18	1.801
CHAP	1 L/min	48 h	full	-10.65	1.813

and 200 μL of fresh DMEM and 50 μL of MTT solution (2 mg/mL in PBS) were added to each well. The cells were then incubated in a 37 °C incubator for 4 h. After removing the MTT solution, 150 μL of DMSO solution was added to each well. The absorbance of the solution in the well was directly read at 540 nm using a SoftMax Pro5 spectrophotometer (Molecular Devices, Sunnyvale, CA, USA). Each assay was repeated six times.

Results and Discussion

Compositional Analysis of CHAP. The CHAP particles were obtained by carbonation of the HAP nano-particles. In the FTIR spectra (Figure 1), the absorption band (963 cm^{-1}) of the phosphate group (PO_4) was decreased by carbonation, whereas the absorption band (880 cm^{-1}) of the carbonate group (CO_3) was increased. This was also confirmed by ICP-MS analysis. The stoichiometric Ca/P ratio of HAP and CHAP was 1.796 and 1.813, respectively. Therefore, the proportion of calcium had been increased by carbonation, whereas that of phosphorus had decreased, indicating that the carbonate group had partially replaced the phosphate group in HAP. The zeta potential decreased from +1.14 mV (in HAP solution) to -10.65 mV (in CHAP solution), indicating that the electric surface potential of the particles had increased in solution, thereby decreasing their cohesion, due to the carbonation.

Figure 2 shows the XRD patterns of the HAP and CHAP

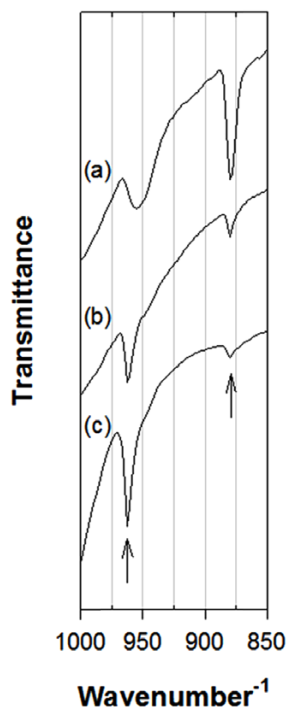


Figure 1. FTIR spectra of bioceramic particles. (a) Carbonated hydroxyapatite (CHAP); (b) intergrade-CHAP; (c) hydroxyapatite (HAP).

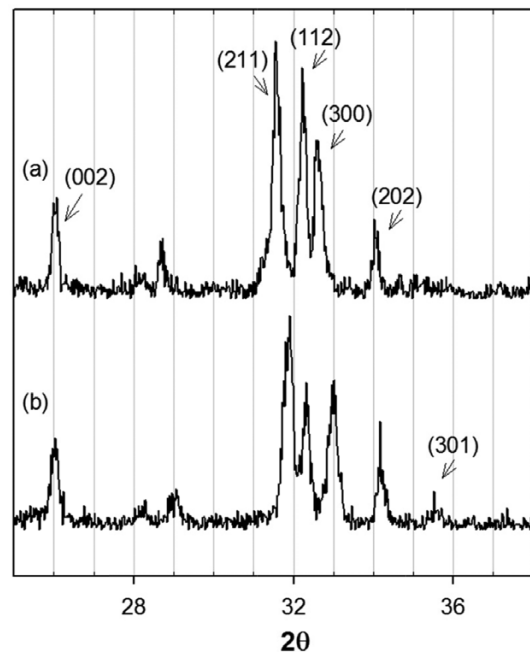


Figure 2. XRD patterns of bioceramic particles. (a) Carbonated hydroxyapatite (CHAP); (b) hydroxyapatite (HAP).

particles. The (211), (112), (300) d-spacing of the hexagonal crystal¹⁶ at $2\theta=31-34^\circ$ were each slightly shifted by carbonation. The crystallinity of HAP and CHAP was calculated at full-width of half-maximum at (002) diffraction, and their crystallite size was calculated at full-width of half-maximum at (211) diffraction using the Scherrer equation as follows:

$$X_c = \left(\frac{K_A}{\beta_{002}} \right), \quad \gamma = \frac{K\lambda}{\beta_{211} \cos \theta}$$

The crystallinity and crystallite size of HAP were 0.35 and 23.36 nm, whereas those of CHAP were 0.79 and 33.09 nm, respectively. The crystallinity and crystallite size of CHAP increased considerably by carbonation.

Structural Analysis of Composites. Figure 3 shows the FTIR spectra of the composites according to chitosan/CHAP ratio. The absorption bands at 1650, 1590, 1565, and 1460 cm^{-1} are the characteristic bands of the amide I (C=O), amino (NH_2), amide II (N-H), and CH_2 groups, respectively.¹⁷ The absorption band of the amino group appeared in the non-acetylated composites (Figure 3(b), (d); indicated by circles), but it disappeared in the acetylated composites. The absorption band of the amide II group appeared in the acetylated composites (Figure 3(a), (c); indicated by triangles). The absorption band close to 1550 cm^{-1} is the characteristic band of the phosphate group of apatite.¹⁶

The XRD patterns of the composites according to ACS/CHAP proportion are shown in Figure 4. The crystalline phase of CHAP was most evident, having specific diffractions at $2\theta=31-34^\circ$. The crystalline phase of chitosan decreased with decreasing chitosan content, and it nearly disappeared in the

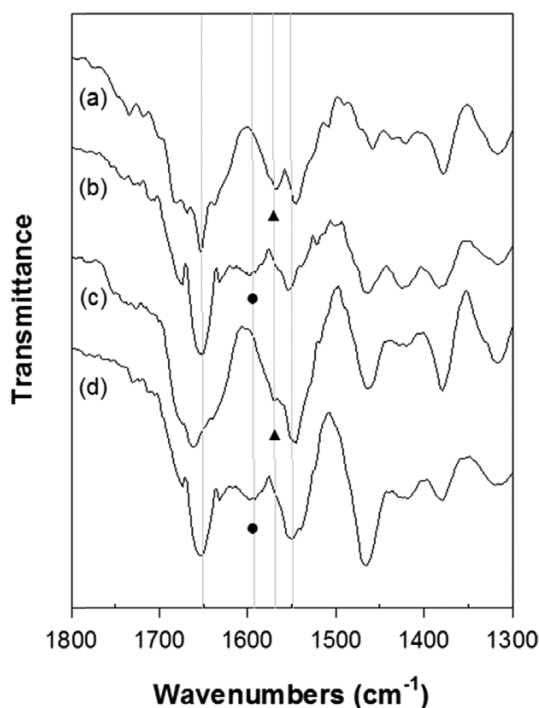


Figure 3. FTIR spectra of chitosan/carbonated hydroxyapatite (CS/CHAP) composites and acetylated chitosan/CHAP (ACS/CHAP) composites. (a) ACS/CHAP=70/30; (b) CS/CHAP=70/30; (c) ACS/CHAP=50/50; (d) CS/CHAP=50/50. ● : 1590 cm^{-1} ; ▲ : 1565 cm^{-1} .

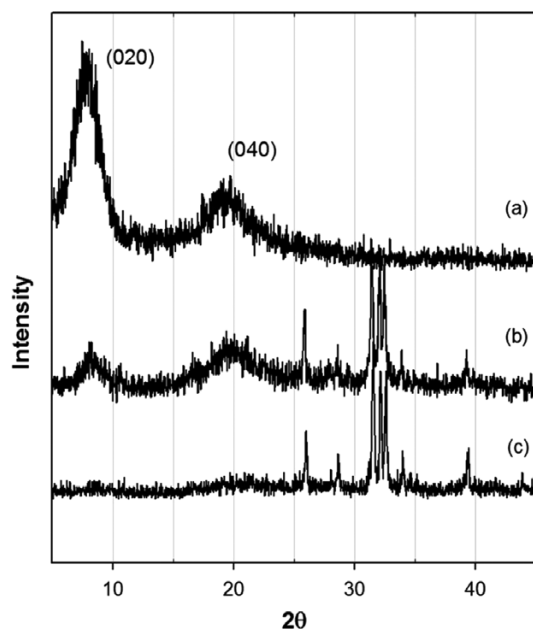


Figure 4. XRD patterns of acetylated chitosan/carbonated hydroxyapatite (ACS/CHAP) composites. (a) ACS/CHAP=100/0; (b) ACS/CHAP=70/30; (c) ACS/CHAP=50/50.

composite ratio of 50/50. It is considered that the CHAP nanoparticles interfered with formation of the crystalline phase of chitosan.

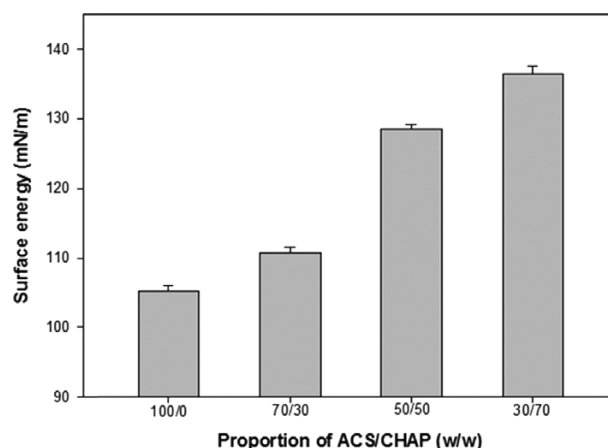


Figure 5. Surface energies of the composites according to the proportion of acetylated chitosan/carbonated hydroxyapatite (ACS/CHAP).

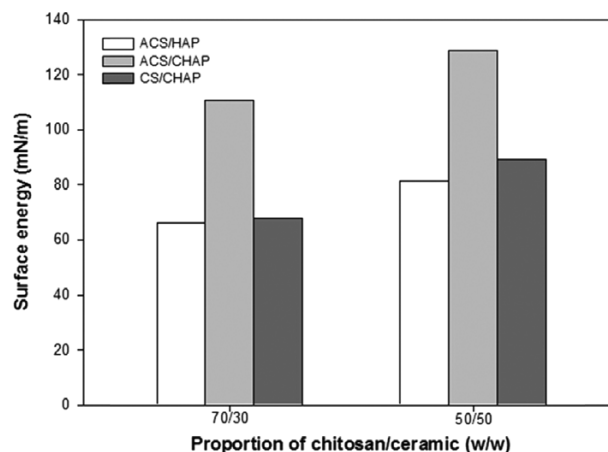


Figure 6. Comparison of the surface energies of the acetylated chitosan/hydroxyapatite (ACS/HAP) composite, ACS/carbonated hydroxyapatite (ACS/CHAP) composite, and chitosan/CHAP (CS/CHAP) composite, caused by acetylation and carbonation.

Surface Energy. The surface energy of a biomaterial is one of the key factors associated with its biological property. Cell adhesion is influenced by the polar component of the material surface.⁵ The surface energy of the composites increased gradually with increasing CHAP proportion in the ACS/CHAP composites (Figure 5), and was also increased by acetylation and/or carbonation (Figure 6). The partial acetylation of chitosan rather increases its hydrophilicity. So when about half of amino groups of chitosan are acetylated, the chitosan become water-soluble. Likewise, it indicates that a partial carbonation of HAP increased the hydrophilicity of the composite.

Water Absorption and Biodegradation. The water absorption capability of a composite is an important factor for interaction of the biomaterial with cells and for the preservation of cell function. Figure 7 shows the water adsorption of the composites according to ACS/CHAP ratio. As the proportion of CHAP

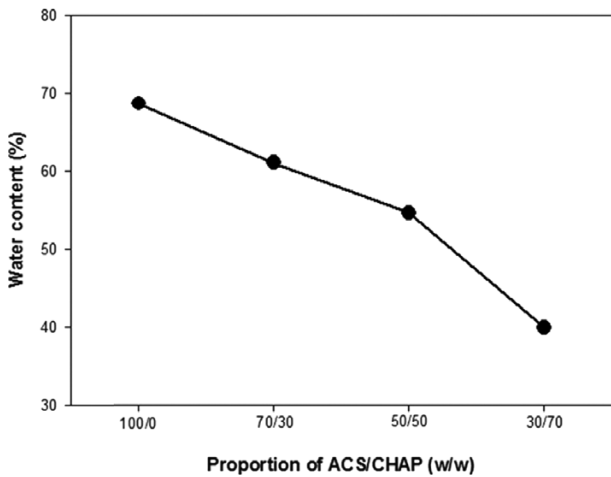


Figure 7. Water absorption ability of the composites according to the proportion of acetylated chitosan/carbonated hydroxyapatite (ACS/CHAP).

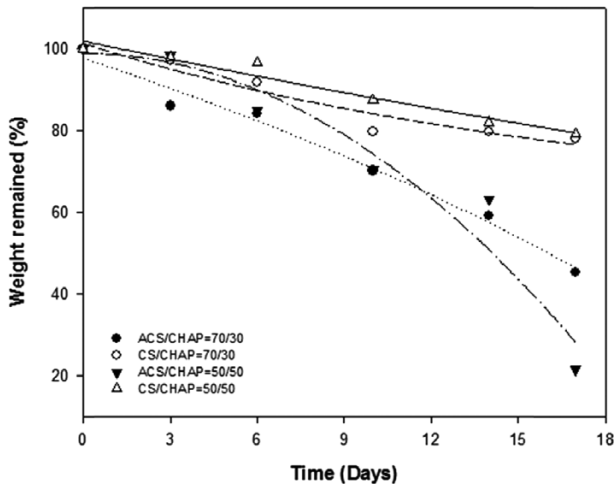


Figure 8. *In vitro* biodegradation of the composites in a PBS solution of lysozyme.

increased, the water absorption decreased proportionally. Xianmiao *et al.*⁶ reported that the swelling ratio of chitosan/HAP composite decreased with the increase of the nano-HAP content. Since the content of polymeric matrix capable of absorbing water had decreased, it was difficult for water to permeate into the composite, and therefore the composite remained in a non-swollen state.

Polysaccharides are generally degraded by enzymatic hydrolysis. Figure 8 shows the *in vitro* degradation of the composites with 4 mg/mL lysozyme. The ACS/CHAP composites were rapidly degraded in comparison with the CS/CHAP composites. The β -1,4 glycosidic linkages of N-acetyl glucosamine tend to be more rapidly hydrolyzed than those of glucosamine. Ko *et al.*¹⁸ reported that the acetylated chitosan sponge was rapidly degraded with increase of acetylation reaction time. Therefore, by increasing the N-acetyl glucosamine/glucos-

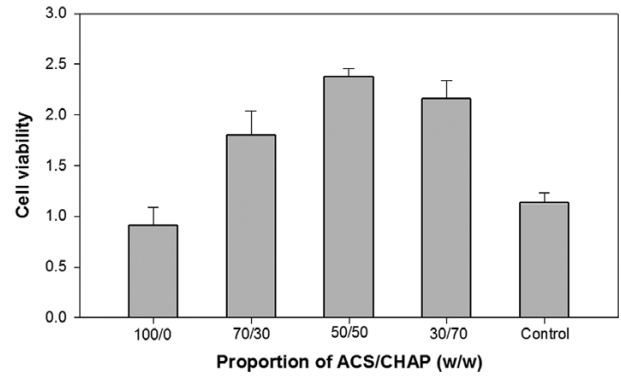


Figure 9. Relative viability of osteoblast-like cells on the composites according to the proportion of acetylated chitosan/carbonated hydroxyapatite (ACS/CHAP).

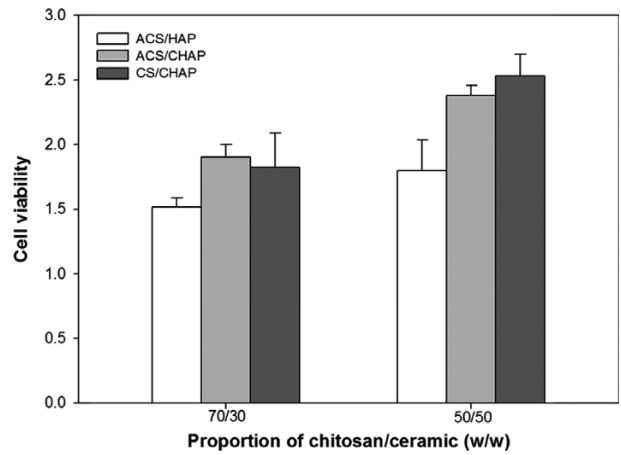


Figure 10. Relative viability of osteoblast-like cells on composites prepared by acetylation and carbonation.

amine ratio of the composite, the degradation of the composite by lysozyme was accelerated.

Cell Viability. The cell viability of osteosarcoma MG-63, an osteoblast-like cell, was estimated by MTT assay. Figure 9 shows the cell viabilities according to ACS/CHAP ratio. Osteosarcoma cells were cultured for 3 days with the composites; commercial polystyrene culture medium was used as the control. The proliferation of osteosarcoma cells on the composite was more pronounced than that on the control. In particular, the highest cell viability occurred in the composite with ACS/CHAP ratio of 50/50, which was about twice that of the control. Biopolymer composites blended with bioceramics generally result in good osteocyte viability and osteoconductivity. It was reported that the proliferation of bone marrow stromal cells was improved in chitosan composite membrane containing HAP.^{12,19} Figure 10 shows the comparison of cell viabilities as a result of carbonation and acetylation of the composites. The relative cell viability on the carbonated composites was higher than that on the non-carbonated composites.

The cell morphologies of osteosarcoma MG-63 cultured

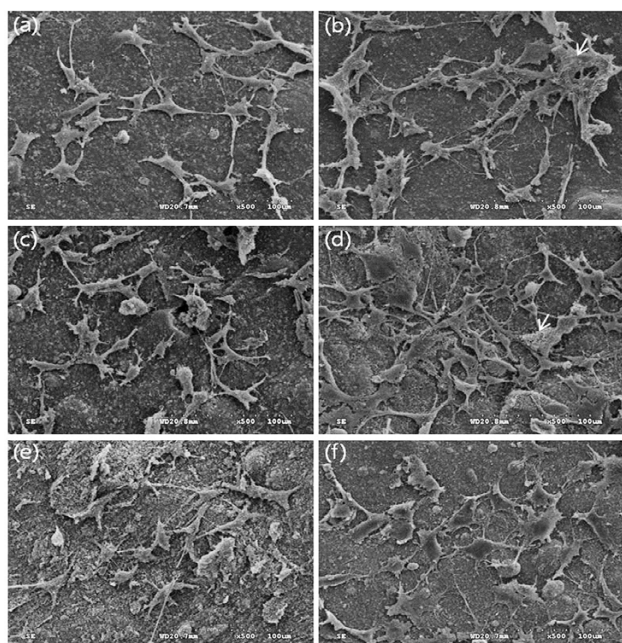


Figure 11. Scanning electron micrographs of the morphology of osteoblast-like MG-63 cells on the surface of the composites after 3 days of culture. Magnification $\times 500$. (a) ACS/CHAP=70/30; (b) CS/CHAP=70/30; (c) ACS/CHAP=50/50; (d) CS/CHAP=50/50; (e) ACS/CHAP=30/70; (f) ACS/HAP=50/50.

for 3 days on the composites are shown in Figure 11. The cells were densely adhered on the 50/50 composites (ACS/CHAP and CS/CHAP). Although the viability and the number of cells on the CS/CHAP composite was slightly more within the margin of error than those on the ACS/CHAP composite, the cells on the non-acetylated composites (CS/CHAP) were partially disrupted and had a two-dimensional spreading flat shape (the arrow on Figure 11(d)), compared with the cells on the acetylated composite (ACS/CHAP). The cells on the HAP composite (ACS/HAP) also showed a spreading flat shape. The normal phenotype was observed on the acetylated composite with carbonated HAP (ACS/CHAP).

Mechanical Property. GBR barriers should have appropriate mechanical properties, such as sufficient strength and

elasticity, to cover spatial bone defects and to block the down-growth of surrounding connective tissues at the implantation region.¹⁻³ Table II shows the mechanical properties of the composites by tensile test. The breaking stress and elongation of the composites decreased with increasing proportion of CHAP. With increase of the ceramic content in the composite, the semicrystalline structure of chitosan collapsed, thereby leading to the brittle nature of the composite.

The acetylated composite (ACS/CHAP) showed slightly lower breaking stress and elongation than the non-acetylated composite (CS/CHAP). The ACS/CHAP composite of 50/50 ratio had a high elastic modulus in spite of the low breaking stress, compared with filter paper as a reference. Therefore, the ACS/CHAP composite of 50/50 was considered to have sufficient mechanical property for a GBR barrier.

Conclusions

In this research, we have developed an improved composite over the current chitosan/hydroxyapatite composite for application as a GBR barrier. The novel composite was prepared by acetylation of the chitosan matrix in which carbonated nano-size HAP particles were dispersed. The components of the composite, CHAP and ACS, are more biomimetic than those of the existing composite, HAP and CS, respectively. The carbonated HAP (CHAP) was obtained by sintering the HAP nano-particles with carbon dioxide. The chitosan/CHAP composites were then acetylated with acetic anhydride. The surface energy of the ACS/CHAP composites was increased by carbonation and acetylation. The water absorption of the composite decreased with increasing CHAP proportion. Acetylation of the composite increased the lysozyme biodegradation of the composite. The viability of osteoblast-like cells was significantly improved on the surface of the carbonated composite. In particular, the high viability and normal phenotype of cells occurred on the ACS/CHAP composite of 50/50 ratio, which had sufficient elastic modulus for a GBR barrier. These results indicate the potential of the biomimetic ACS/CHAP composite for use as an improved barrier for GBR.

Table II. Mechanical Properties of the Composites

	Ratio	Stress at Break (MPa)	Elongation (%)	Elastic Modulus (MPa)
ACS/CHAP Composites	100/0	26.77	1.89	1416.51
	70/30	10.98	1.16	946.84
	50/50	2.84	0.63	451.41
	30/70	0.88	0.63	140.09
CS/CHAP Composites	70/30	11.67	1.85	630.80
	50/50	3.04	0.63	482.55
Reference	Filter Paper	6.67	1.85	360.46

Acknowledgment. This work was supported by a 2-Year Research Grant of Pusan National University

References

- (1) Y. Meng, M. Liu, S. A. Wang, A. C. Mo, C. Huang, Y. Zuo, and J.-D. Li, *Appl. Surf. Sci.*, **255**, 267 (2008).
- (2) M. Taba Jr, Q. Jin, J. V. Sugai, and W. V. Giannobile, *Orthod. Craniofac. Res.*, **8**, 292 (2005).
- (3) M. Ito, Y. Hidaka, M. Nakajima, H. Yagasaki, and A. H. Kafrawy, *J. Biomed. Mater. Res.*, **45**, 204 (1999).
- (4) C. Y. Choi, S. B. Kim, P. K. Pak, D. I. Yoo, and Y. S. Chung, *Carbohydr. Polym.*, **68**, 122 (2007).
- (5) Y. Zhang and M. Zhang, *J. Mater. Sci. Mater. Med.*, **15**, 255 (2004).
- (6) C. Xianmiao, L. Yubao, Z. Yi, Z. Li, L. Jidong, and W. Huanan, *Mater. Sci. Eng. C*, **29**, 29 (2009).
- (7) A. Lahiji, A. Sohrabi, D. S. Hungerfordand, and C. G. Frondoza, *J. Biomed. Mater. Res.*, **51**, 586 (2000).
- (8) R. Murugan and S. Ramakrishna, *Biomaterials*, **25**, 3829 (2004).
- (9) H. S. Kim, J. T. Kim, Y. J. Jung, S. C. Ryu, H. J. Son, and Y. G. Kim, *Macromol. Res.*, **15**, 65 (2007).
- (10) A. N. Koo, J.-Y. Ohe, D.-W. Lee, J. Chun, H. J. Lee, Y.-D. Kwon, and S. C. Lee, *Macromol. Res.*, **23**, 1168 (2015).
- (11) S. A. Park, J. B. Lee, Y. E. Kim, J. E. Kim, J. H. Lee, J.-W. Shin, I. K. Kwon, and W. D. Kim, *Macromol. Res.*, **22**, 882 (2014).
- (12) J. M. Song, S. H. Shin, Y. D. Kim, J. Y. Lee, Y. J. Baek, S. Y. Yoon, and H. S. Kim, *Int. J. Oral Sci.*, **6**, 87 (2014).
- (13) Y.-H. Kang, H.-C. Kim, S. H. Shin, H. S. Kim, K.-C. Kim, and S.-H. Lee, *Tissue Eng. Regen. Med.*, **8**, 23 (2011).
- (14) J. Xu, S. P. McCarthy, R. A. Gross, and D. L. Kaplan, *Macromolecules*, **29**, 3436 (1996).
- (15) E. Landi, G. Celotti, G. Logroscino, and A. Tampieri, *J. Eur. Ceram. Soc.*, **23**, 2931 (2003).
- (16) A. Ślósarczyk, Z. Paszkiewicz, and C. Paluszkiwicz, *J. Mol. Struct.*, **744-747**, 657 (2005).
- (17) H. S. Kim, J. T. Kim, Y. J. Jung, D. Y. Hwang, H. J. Son, J. B. Lee, S. C. Ryu, and S. H. Shin, *Macromol. Res.*, **17**, 682 (2009).
- (18) J. A. Ko, B. K. Kim, and H. J. Park, *J. Appl. Polym. Sci.*, **117**, 1618 (2010).
- (19) S.-H. Lee, B.-J. Kim, S.-H. Shin, H. S. Kim, K.-C. Kim, C.-H. Kim, Y.-H. Kang, and J.-B. Jo, *Tissue Eng. Regen. Med.*, **6**, 916 (2009).